The crystal structure of the ligand-binding module of human TAG-1 suggests a new mode of homophilic interaction

MARIO MÖRTL,[1] PETER SONDEREGGER,[2] KAY DIEDERICHS,[1] AND WOLFRAM WELTE[1]

[1]University of Konstanz, Department of Biology, D-78464 Konstanz, Germany
[2]University of Zürich, Department of Biochemistry, CH-8057 Zürich, Switzerland

(RECEIVED May 4, 2007; FINAL REVISION July 10, 2007; ACCEPTED July 10, 2007)

Abstract

Human TAG-1 is a neural cell adhesion molecule that is crucial for the development of the nervous system during embryogenesis. It consists of six immunoglobulin-like and four fibronectin III-like domains and is anchored to the membrane by glycosylphosphatidylinositol. Herein we present the crystal structure of the four N-terminal immunoglobulin-like domains of TAG-1 (TAG-$1_{Ig1–4}$), known to be important in heterophilic and homophilic macromolecular interactions. The contacts of neighboring molecules within the crystal were investigated. A comparison with the structure of the chicken ortholog resulted in an alternative mode for the molecular mechanism of homophilic TAG-1 interaction. This mode of TAG-1 homophilic interaction is based on dimer formation rather than formation of a molecular zipper as proposed for the chicken ortholog.

Keywords: protein structure; cell adhesion; TAG-1; buried surface

Cell adhesion molecules (CAMs) play a crucial role during the development of the nervous system. They are found on the neuronal somas, on the dendrites, and the axons and their growth cones; they can also be found as components of glial cells, the extracellular matrix, and in soluble form in the interstitial space (Dodd and Jessell 1988; Jessell 1988; Tessier-Lavigne and Goodman 1996). Neural CAMs have been grouped into different families on the basis of the domain composition of their extracellular part. Several important neural CAMs belong to the immunoglobulin superfamily (IgSF). Prominent representatives of this category, including TAG-1, L1, and NgCAM, are composed of repeated immunoglobulin (Ig)-like and fibronectin III (FnIII)-like domains (Chothia and Jones 1997). They guide developing axons, by mediating adhesive cell–cell and cell–matrix interactions and by recognizing and transducing growth signals from the environment (Rathjen and Jessell 1991; Hynes and Lander 1992; Brümmendorf and Rathjen 1996). The human transient axonal glycoprotein TAG-1 belongs to the contactin family of IgSF CAMs, which comprises proteins with six N-terminal Ig and four FnIII domains attached to the cell membrane by a glycosylphosphatidylinositol anchor (Hasler et al. 1993; Tsiotra et al. 1993). Orthologs of human TAG-1 (also known as TAX1) are found in mouse, rat, and chicken (axonin-1) (Yamamoto et al. 1986; Dodd et al. 1988; Stoeckli et al. 1989). An interesting feature of TAG-1 is the maintenance of their ligand-binding characteristics across the species border. This functional similarity between different species was exploited in several studies, where heterophilic binding was studied between binding partners originating from different species (Tsiotra et al. 1993; Milev et al. 1996;

Reprint requests to: Wolfram Welte, Department of Biology, University of Konstanz, Fach M656, Universitätsstrasse 10, D-78464 Konstanz, Germany; e-mail: wolfram.welte@uni-konstanz.de; fax: +49-7531-883183.

Abbreviations: IgSF, immunoglobulin superfamily; Ig domain, immunoglobulin-like domain; FnIII domain, fibronectin III-like domain; CV, column volume(s); B, buried surface; $f_{np}B$, nonpolar interface area; f_{bu}, fraction of fully buried atoms; RP, residue propensity score; S_C, shape complementarity value; R_{work} or R_{free}, R factor (defined in Table 2).

Article published online ahead of print. Article and publication date are at http://www.proteinscience.org/cgi/doi/10.1110/ps.072802707.

De Angelis et al. 1999; Pavlou et al. 2002). This indicates that these molecules have not lost or changed their function in the development of the nervous system during evolution between humans, rodents, and birds, allowing the direct comparison of results obtained from experiments with orthologous molecules.

Other important IgSF CAMs are the transmembrane proteins L1, NgCAM, and NrCAM, which belong to the L1 family (Moos et al. 1988; Burgoon et al. 1991). They are composed of four Ig and five FnIII domains, a transmembrane helix, and a small intracellular domain (Grumet and Edelman 1984; Lemmon et al. 1989; Grumet et al. 1991). Many IgSF CAMs are known to interact with macromolecular partners both in the same membrane (*cis*) and across the intracellular space from one cell to the other (*trans*).

TAG-1 was initially described and purified as an axonally secreted protein of dorsal root ganglia neurons (Stoeckli et al. 1989) and is transiently expressed during the development of the central and peripheral nervous systems as a glycosylphosphatidylinositol-anchored and as a secreted form (Dodd et al. 1988; Karagogeos et al. 1991; Stoeckli et al. 1991). Recent studies have shown that TAG-1 is expressed by corticofugal axons, where it serves as a substrate for migrating cortical interneurons, and that its expression is regulated by thyroid hormone (Alvarez-Dolado et al. 2001; Denaxa et al. 2001). TAG-1 has also been implicated in axon–glia interactions and is probably involved in the tumorigenesis of malignant gliomas (Suter et al. 1995; Rickman et al. 2001; Traka et al. 2002).

TAG-1 can act as heterophilic binding partner for several neural CAMs belonging to different structural categories, including NgCAM or L1, NrCAM, contactin/F11/F3, β-integrin, Neurocan, Phosphacan/RPTP-ζ/β, and NCAM (Kuhn et al. 1991; Felsenfeld et al. 1994; Buchstaller et al. 1996; Milev et al. 1996; Buttiglione et al. 1998; Malhotra et al. 1998; Lustig et al. 1999). The binding of TAG-1 to NgCAM and NrCAM is mediated by the four N-terminal Ig domains (Kunz et al. 1998; Fitzli et al. 2000), which form a structural entity called the ligand-binding module that can maintain its structural and functional integrity only in the presence of all four N-terminal domains (this work and Rader et al. 1996; Freigang et al. 2000).

Apart from the ability to interact heterophilically with other AxCAMs and with extracellular matrix compounds, TAG-1 and its orthologs are able to interact homophilically. Chicken TAG-1 expressed on myeloma cells as well as human TAG-1 expressed on S2 cells have the ability to induce cell–cell aggregation by a *trans* interaction of TAG-1 (Rader et al. 1993; Tsiotra et al. 1996; Kunz et al. 2002). The crystal structure of chicken TAG-1 revealed important information to narrow down the region on the four N-terminal Ig domains responsible for homophilic TAG-1 interaction (Freigang et al. 2000). Analysis of the crystal packing together with site-directed mutagenesis experiments resulted in a zipper-like model for the homophilic interaction of TAG-1 in aggregating myeloma cells (Freigang et al. 2000). Here, we report on the crystal structure of human TAG-1. We present indications for an alternative mode of homophilic *trans* interaction, which is equally in accordance with the mutagenesis results of Freigang and colleagues (Freigang et al. 2000).

Results

Refolding and purification

Expression of TAG-$1_{Ig1–4}$ in 1 L culture yielded 2 mg of denatured and purified protein after the metal-affinity column. After initiation of refolding by dilution, TAG-$1_{Ig1–4}$ was checked daily for its apparent molecular mass by SDS-PAGE. Oxidation of all four disulfide bonds of TAG-$1_{Ig1–4}$ was indicated by a shift from ~45 kDa to ~40 kDa due to the formation of four disulfide bonds. After 7 days, the cysteines were fully oxidized. By gel filtration prior to crystallization, 0.1 mg of monomeric, oxidized, purified TAG-$1_{Ig1–4}$ per liter of culture was obtained.

Crystallization, structure determination, and refinement

Needle-like crystals of TAG-$1_{Ig1–4}$ grew within 2 weeks to a size of $5 \times 5 \times 70$ μm^3 and belonged to space group $C222_1$ with one molecule per asymmetric unit. Data processing statistics are summarized in Table 1.

Molecular replacement (MOLREP) with chicken TAG-1 (PDB code 1CS6) as a search model was successful to obtain initial phases. The final structure of TAG-$1_{Ig1–4}$ had an overall root mean square (RMS) deviation of 1.52 $Å^2$ from the search model. Refinement with COOT and REFMAC yielded final R_{work}/R_{free} values of 23.5%/27.9%. After the refinement procedure, reasonable geometrical

Table 1. *Data collection statistics of TAG-$1_{Ig1–4}$*

Data set	TAG-1 native
Wavelength (Å)	1.07068
Resolution (Å)	20–3.1 (3.26–3.07)[a]
Unique reflections	7518 (950)
Completeness (%)	94.9 (76.7)
Average I/σ	12.9 (2.2)
R_{mrgd-f} (%)[b]	11.4 (59.7)
Space group	$C222_1$
Cell dimensions (Å)	$a = 46.7$, $b = 106.8$, $c = 161.3$

[a] Values in parentheses correspond to the highest-resolution shell.
[b] See Diederichs and Karplus (1997).

Table 2. *Refinement statistics of TAG-$1_{Ig1–4}$*

Resolution (Å)	19.5–3.07
Total no. of non-hydrogen atoms	2895
Total no. of reflections	7090
No. of reflections in test set	452
R_{work} (%)[a]	23.5
R_{free} (%)[b]	27.9
RMS distance from ideal geometry	
Bonds (Å)	0.007
Angles (°)	1.078
Ramachandran plot[c]	
Most-favored regions	272(86.1%)
Additionally allowed regions	37(11.7%)
Generously allowed regions	3(0.9%)
Disallowed regions	4(1.3%)
No. of non-glycine, non-proline, and non-end residues	316(100%)
No. of glycine, proline, and end residues	55
Total no. of residues[d]	371

[a] R factor $= \Sigma_{hkl}||F_{obs}| - k|F_{calc}||/\Sigma_{hkl}|F_{obs}|$, where F_{obs} and F_{calc} are the observed and calculated structure factors.
[b] For R_{free}, the sum is extended over a subset of reflections, excluded from all stages of refinement.
[c] See Laskowski et al. (1993).
[d] Residues 247–256 were excluded from refinement because this region has no visible electron density.

values were obtained (see Table 2). For a detailed electron density map around the Cys31–Cys81 disulfide bond, see Figure 1.

U-shaped arrangement of the four N-terminal Ig domains of TAG-$1_{Ig1–4}$

The four Ig domains of human TAG-$1_{Ig1–4}$ are arranged as a compact module (see Fig. 2), which allows strong interaction between the Ig1 and Ig4 domains as well as between the Ig2 and Ig3 domains. The U-shaped overall structure was already predicted (Rader et al. 1996) and reported (Freigang et al. 2000) for the chicken ortholog. A similar U-shaped arrangement of four Ig domains is shared also by the distantly related molecule hemolin from of the immune system of the giant silk moth *Hyalophora cecrophia* (Su et al. 1998). Other CAMs of the F11 family (F11, F3) and the L1 family (L1, NgCAM, and NrCAM) also have this elongated linker. Compared to TAG-1, the NgCAM-related cell adhesion molecule NrCAM has 20 additional residues within the linker region, whereas the other molecules have no significant change in the length of their linkers. A shorter linker than in TAG-1 probably would not allow a bend after the Ig2 domain, which is required for the interaction between Ig2 and Ig3 domain in human and chicken TAG-1 and hemolin. In contrast, L1 may possess two different spatial arrangements of the four N-terminal Ig domains, one with an U-shaped domain arrangement, as reported here for TAG-$1_{Ig1–4}$, and an extended conformation, where the four N-terminal Ig-domains do not form a compact module (Schürmann et al. 2001).

A comparison between human TAG-$1_{Ig1–4}$, chicken TAG-$1_{Ig1–4}$, and hemolin$_{Ig1–4}$ showed, that the root mean square (RMS) deviation of the domain pairs Ig1:Ig4 as well as Ig2:Ig3 is lower than the overall RMS deviation of the whole molecules. The RMS deviation between human and chicken TAG-$1_{Ig1:Ig4}$ is 0.82 Å; between human and chicken TAG-$1_{Ig2:Ig3}$, 0.75 Å; between the whole molecules TAG-$1_{Ig1–4}$ of both organisms, 1.52 Å. This indicates a tight interaction of the Ig domains within the pairs Ig1:Ig4 and Ig2:Ig3 and the existence of two hinge joints, located between Ig1 and Ig2 domains and between Ig3 and Ig4 domains. A comparison of human TAG-$1_{Ig1–4}$ with the chicken ortholog, using the program DYNDOM (Hayward and Lee 2002) located the residues of the hinge joints accordingly at the residues Leu^{102} and Gln^{296}. This suggests that the tertiary structure of TAG-$1_{Ig1–4}$ can be seen as composed of two rigid groups: Ig1:Ig4 domains and Ig2:Ig3 domains. A similar comparison of human and chicken TAG-$1_{Ig1–4}$ with hemolin$_{Ig1–4}$ gave further evidence for the two hinges.

Intermolecular β-strand pairing stabilizes the largest lattice contact between two TAG-$1_{Ig1–4}$ molecules

Despite the structural similarity of human and chicken TAG-$1_{Ig1–4}$, the arrangement within the corresponding crystal lattice showed differences, which may be important to understand the molecular mechanism of homophilic interaction. The investigation of the lattice contacts of chicken TAG-$1_{Ig1–4}$ resulted in a model for homophilic TAG-1 interaction which was supported by two mutants

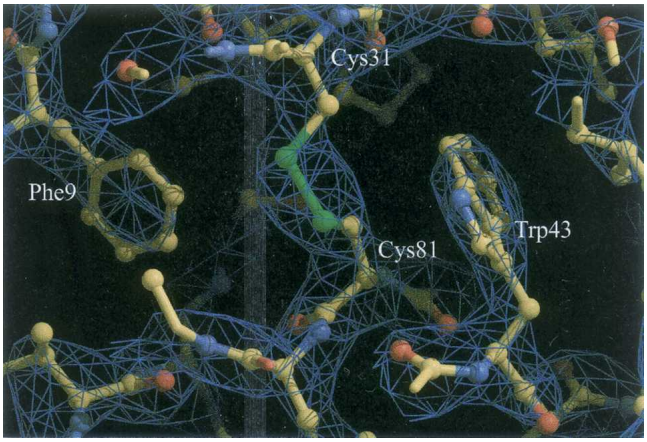

Figure 1. Detail of the electron density map: 2σ cut of the σ-weighted $2F_{obs} - F_{calc}$ map near the disulfide bond of Cys31–Cys81. The figure was produced with COOT (Emsley and Cowtan 2004) and Raster3D (Merritt and Bacon 1997).

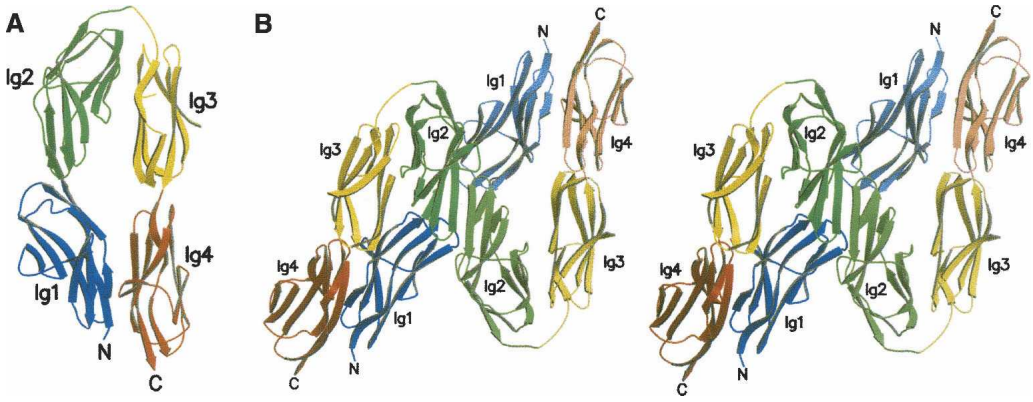

Figure 2. Domain arrangement and groove to groove interaction of TAG-$1_{Ig1–4}$. (*A*) Overall structure of human TAG-$1_{Ig1–4}$. The four N-terminal Ig domains of human TAG-1 are arranged in a U-like manner. The elongated linker between the Ig2 and Ig3 domain allows apposition of the Ig3 and Ig4 domains to the Ig1 and Ig2 domains, respectively. Specific interactions between Ig1 and Ig4, as well as between Ig2 and Ig3, stabilize the quaternary structure of the so-called ligand-binding module. Ig pairs Ig1:Ig4 and Ig2:Ig3 form two rigid groups connected by a hinge, located at the residues Leu^{102} and Gln^{296}, which are found at the linkers between Ig1 to Ig2 and between Ig3 to Ig4, respectively. Residues 247–256 could not be modeled because density was lacking. (*B*) Stereoview of the dimer of two TAG-1 ligand-binding modules. The TAG-$1_{Ig1–4}$ interaction site is located at the groove near the Ig1–Ig2 linker. Both molecules contact each other via their G strands (for details see Fig. 3A). This figure was produced using the programs MOLSCRIPT (Kraulis 1991) and Raster3D (Merritt and Bacon 1997).

of the chicken ortholog with mutations located on the FG loop of the Ig2 domain. The deletion of residues Ile^{187} to Ile^{190} as well as the combined exchange of His^{186} and Phe^{189} to alanine residues were sufficient to abolish myeloma cell–cell aggregation (Freigang et al. 2000). In the human TAG-$1_{Ig1–4}$ crystal structure, the lattice contact burying the largest surface (2240 $Å^2$) is composed of surface parts from Ig1 and Ig2 domains. Both molecules contact each other along the groove near the Ig1–Ig2 linker (see Fig. 2B). The FG loop of the Ig2 domain is also part of this lattice contact which therefore has to be considered as a potential protein interaction site. All other lattice contacts buried surfaces corresponding to average crystal lattice contacts (570 $Å^2$ for simple lattice contacts, see Janin 1997; 1350 $Å^2$ for lattice contacts with twofold symmetry, see Janin and Rodier 1995).

In contrast to the largest lattice contact found in the chicken ortholog, the two contacting human TAG-$1_{Ig1–4}$ molecules are related by twofold crystallographic symmetry. The rotation axis passes between adjacent G strands connected by six hydrogen bonds of the following backbone amino and carbonyl groups: $Phe^{185\prime}$O and $Phe^{191\prime\prime}$N; $Thr^{187\prime}$N and $Ser^{189\prime\prime}$O; $Thr^{187\prime}$O and $Ser^{189\prime\prime}$N; $Ser^{189\prime}$N and $Thr^{187\prime\prime}$O; $Ser^{189\prime}$O and $Thr^{187\prime\prime}$N; and $Phe^{191\prime}$N and $Phe^{185\prime\prime}$O. The apposition of both G strands thus results in an intramolecular antiparallel β-sheet (Figs. 2B, 3). The two residues, Phe^{185} and Thr^{187}, which are involved in the formation of the six hydrogen bonds of both participating β-strands, are in the elongated region of the FG loop, which is missing in the three other Ig domains. In addition these central β-strands are framed by hydrophobic areas, which are formed mainly by the aromatic side chains of Phe^{143}, Phe^{191}, and Phe^{194} (see Fig. 3). These three residues stabilize each other and provide a hydrophobic pocket for the phenyl group of Phe^{185} of the corresponding dimer mate (see Fig. 3). The relevant distances of the phenylalanine side chains are in the range of 5.3–6.6 Å. This packing meets the characteristics of aromatic–aromatic interactions which are often found in the hydrophobic core of globular proteins (Burley and Petsko 1985).

Another region contributing to the dimer interface is the segment from Glu^{21} to Glu^{24} from Ig1 which approaches the segment from Gln^{104} to Lys^{107} of Ig2 domain of the symmetry-related molecule, but a detailed analysis of the interacting residues and its side chains is not possible because the side-chain density does not allow further interpretation. Only an overall interlocking conformation of the participating TAG-$1_{Ig1–4}$ segments can be recognized.

The mode of TAG-$1_{Ig1–4}$ dimerization proposed in this work and the mode of oligomerization proposed for the chicken ortholog (Freigang et al. 2000) both involve the same residues from β-strands F and G of the Ig2 domain. Each molecule contributes the same part of its surface to the homophilic dimer because of the crystallographic twofold symmetry. However, the proposed oligomerization mechanism of the chicken ortholog is fundamentally different, because the interaction of two molecules involves different residues from both partners: The FG loop of the Ig2 domain of one molecule interacts with a protruding loop located between the β-strands C and E

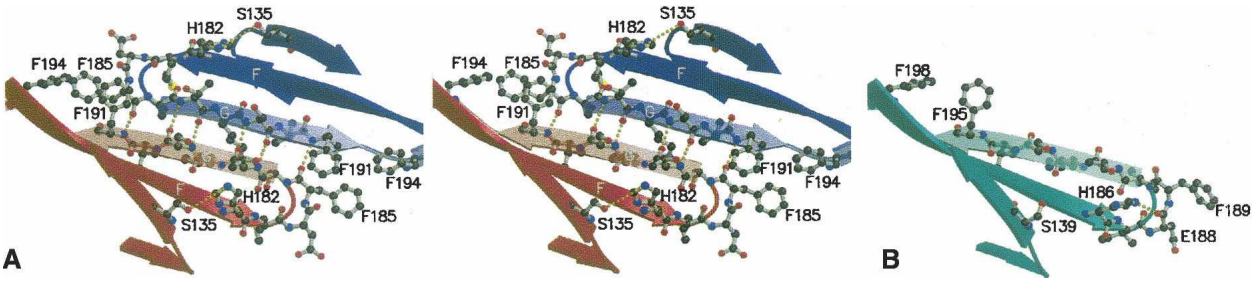

Figure 3. The largest TAG-1 lattice contact. (*A*) Stereoview: The antiparallel β-sheet of the crystallographic human TAG-$1_{Ig1–4}$ dimer is formed by apposition of two Ig2 G strands of TAG-$1_{Ig1–4}$ symmetry mates. The six intermolecular hydrogen bonds, which contribute to the stability of the dimer, are indicated by dotted lines. On both ends of the contacting β-strands G^{blue} and G^{red} are hydrophobic pockets, each formed by Phe^{185}, Phe^{191}, and Phe^{194}. On the *bottom* of the red molecule are shown two hydrogen-bonded residues, Ser^{135} and His^{182}. Phe^{143}, which is part of the hydrophobic patch, is not shown. (*B*) Detailed view of the Ig2 FG residues of chicken TAG-1 for comparison in the same orientation as the red molecule of Figure 2A. Mutations that abolished myeloma cell–cell aggregation were targeted here: His^{186} and Phe^{189} point mutations to alanine as well as a deletion mutant, lacking the four residues Ile^{187}–Ile^{190} (Freigang et al. 2000). This figure was produced using the programs MOLSCRIPT (Kraulis 1991) and Raster3D (Merritt and Bacon 1997).

of the Ig3 domain from another molecule. This kind of interaction results in a string of interacting molecules, arranged in a zipper-like manner (see Fig. 4A for a schematic diagram). The chicken TAG-1 zipper model requires that the interaction sites from adjacent molecules are different, whereas the dimer proposed herein for the human ortholog results in a pairwise interaction, involving identical interaction sites of each dimer mate.

As mentioned previously, the residues of the FG loop from the Ig2 domain are important in both models. A clear difference between the chicken and human TAG-$1_{Ig1–4}$ structure is the stabilization of the FG loop by the residue His^{182}. In human TAG-$1_{Ig1–4}$, His^{182} is hydrogen bonded to the side chain of Ser^{135} (see Fig. 3), whereas in the chicken ortholog, the corresponding residue is hydrogen bonded to the carbonyl group of Glu^{188}. Although the histidine side chains in both models differ by a rotation of almost 180°, both FG loops have a very similar conformation.

A detailed analysis of human and chicken TAG-$1_{Ig1–4}$ crystal lattices classifies the largest lattice contact of the human ortholog as a protein interaction site

In human TAG-$1_{Ig1–4}$, the largest surface of a lattice contact is 2240 $Å^2$, which is almost twice as large as the largest one of the chicken counterpart (1271 $Å^2$). Buried surfaces of lattice contacts and of protein interaction sites show large variations, but an area above 1200 $Å^2$ was proposed as characteristic of specific protein interaction sites (Janin 1997). Because buried surface areas of protein interaction sites and lattice contacts overlap, additional criteria must be used to distinguish between both. S_C, $f_{np}B$, f_{bu}, and RP were calculated here. The

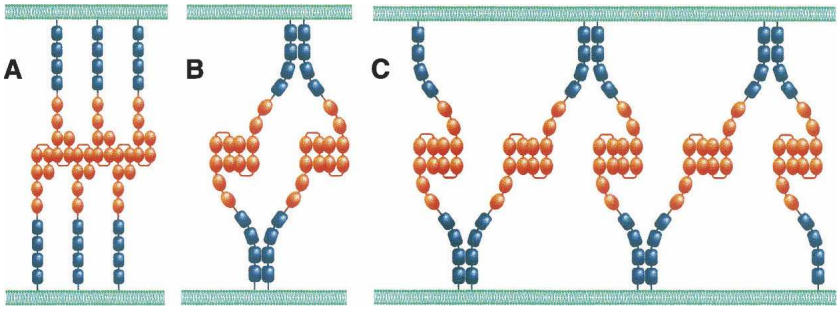

Figure 4. Comparison of putative TAG-1 cell–cell interaction modes; N-terminal Ig domains are indicated in red, and C-terminal FnIII domains are in blue. All TAG-1 molecules are GPI-anchored in the cell membrane by the fourth FnIII domain. (*A*) Zipper mode, as proposed for chicken TAG-$1_{Ig1–4}$ (Freigang et al. 2000). All molecules have two different protein interaction sites, which are located on the Ig2 and Ig3 domains, respectively. (*B*) The *four molecule mode* is the smallest possible *trans–cis* complex in accordance with the crystallographic dimer of human TAG-$1_{Ig1–4}$, where all molecules are involved in *trans* and *cis* interactions simultaneously. (*C*) The *multiple molecule mode* is a generalization of *B*, where many molecules participate in a linear arrangement. The flexibility between *cis* and *trans* binding sites allows a curvilinear arrangement of consecutive TAG-1 dimers, which is not implied by the schematic view.

combination of $f_{np}B$, f_{bu}, and RP was found to allow discrimination between especially large lattice contacts (>800 Å^2) and protein interaction sites (Bahadur et al. 2004). The shape complementarity value (S_C) (Lawrence and Colman 1993) is used to check how well two adjacent surfaces fit together by taking into account distances and angles between both surfaces. The calculated S_C values were 0.70 for the human TAG-$1_{Ig1–4}$ homophilic dimer and 0.63 for the zipper model of the chicken ortholog. A comparison with known protein interaction sites (S_C = 0.70–0.78) and antibody–antigen complexes (S_C = 0.62–0.68) (Lawrence and Colman 1993) shows that the S_C value of the human TAG-$1_{Ig1–4}$ homophilic dimer is in the range of known protein interaction sites, whereas in the chicken ortholog it is in the range of antibody–antigen complexes. Using the three values $f_{np}B$, f_{bu}, and RP, which do not correlate with the size (B) of the interface, as well as the combination of these values according to Bahadur et al. (2004), classifies the dimer interface of the human ortholog as a protein interaction site and the chicken TAG-$1_{Ig1–4}$ zipper interface as a lattice contact. For human TAG-$1_{Ig1–4}$, the following values were determined: $f_{np}B$ = 1282, f_{bu} = 0.24, and RP = 3.14; and for the chicken counterpart, $f_{np}B$ = 740, f_{bu} = 0.15, and RP = −0.91. According to Bahadur et al. (2004), the combination of $f_{np}B$ and f_{bu} were sufficient to classify the chicken TAG-$1_{Ig1–4}$ zipper interface as a lattice contact. In the case of human TAG-1, the combination of $f_{np}B$, f_{bu}, and the large RP value (RP = 3.14) classified the observed dimer interface as a protein interaction site.

Discussion

The binding module of TAG-1 is composed of two rigid groups

The U-shaped arrangement of the four N-terminal Ig domains of human TAG-1 was also found in the chicken ortholog and moth hemolin, with minor differences in the relative orientation of the single Ig domains. Comparison of RMS deviations showed that the binding module is composed of two rigid groups, each formed by two Ig domains: Ig1:Ig4 and Ig2:Ig3, which are connected by two hinges between Ig1 and Ig2 and between Ig3 and Ig4. The crystallographic TAG-$1_{Ig1–4}$ dimer with the largest interface area is formed by molecules which interact along the groove formed by the Ig1–Ig2 linker. The existence of two rigid groups within the binding module may reflect the importance of a correct hinge angle as a prerequisite for TAG-1 dimerization. Two hinge joints as found here between both rigid groups of the binding module restrict the movement of both groups to a flapping movement around the hinge axis.

Largest lattice contact of TAG-$1_{Ig1–4}$ hints at an alternative mode of homophilic interaction

As mentioned in a previous section, human and chicken TAG-1 are similar not only with respect to the overall structure of the four N-terminal Ig domains but also with respect to biochemical behavior in cellular assays, where TAG-1 as well as its binding partners can be replaced by its corresponding orthologs and vice versa (Tsiotra et al. 1993; Milev et al. 1996; De Angelis et al. 1999; Pavlou et al. 2002). This ability to substitute different molecules within the same experiment must reflect structural similarity and suggests that the mechanisms for homophilic interaction of human TAG-1 as well as its chicken and rodent counterparts are similar. The zipper model proposed by (Freigang et al. 2000) and the dimer model proposed herein for homophilic interaction of the binding module are different. An important region for aggregation of myeloma cells by homophilic interaction of chicken TAG-1 was identified at the FG loop of the Ig2 domain (Freigang et al. 2000), which is involved in the largest lattice contact of both, human and chicken TAG-$1_{Ig1–4}$ crystals. In the case of the human ortholog, the dimer with the largest buried surface is formed by intermolecular β-strand pairing of the two Ig2 G strands from different molecules. An intermolecular β-sheet is formed by both dimer mates, which are related by twofold crystallographic symmetry. However, in the chicken ortholog, the zipper formation is due to interaction of the Ig2 FG loop with the extended Ig3 CE loop, and contacting molecules are related by a crystallographic twofold screw axis.

Because both interaction modes seem to be mutually exclusive but in accordance with the mutagenesis experiments of Freigang et al. (2000), they were compared carefully. Parameters were used which can help to discriminate between lattice contacts and specific protein interaction sites. The interface area B and the shape complementarity value S_C are both larger for the interface of human TAG-$1_{Ig1–4}$. In antigen–antibody complexes, both parameters have values which lie between lattice contacts and protein interaction sites (B = 1500 ± 250 Å^2); (see Janin 1997); (S_C = 0.64–0.68); (see Lawrence and Colman 1993). The B and S_C values of human TAG-$1_{Ig1–4}$ are larger and the values for the chicken ortholog are smaller than the values for antibody–antigen complexes. Both values thus favor the model derived from the human TAG-1 structure over the zipper model, derived from the chicken ortholog. The nonpolar interface area ($f_{np}B$), the fraction of fully buried atoms (f_{bu}), and the residue propensity score (RP) (Bahadur et al. 2004) gave further support for the human TAG-1–derived dimer model, because the human TAG-$1_{Ig1–4}$ dimer interface was classified as a specific protein interaction, whereas the zipper interface of the chicken ortholog was classified as a lattice

contact. Conclusions about the in vivo situation can be wrong, because the classification procedure was correct for a distinct fraction of tested interfaces only. Statistically 7% of validated protein interaction sites are classified as lattice contacts (false negatives) using the $f_{np}B/f_{bu}$/RP classification. The same fraction (7%) of false negatives was found for validated crystal lattice contacts with twofold symmetry, wrongly classified as protein interaction sites (Bahadur et al. 2004).

A closer view on those residues in the human ortholog, which correspond to the mutagenesis experiments of Freigang et al. (2000), shows that both combinations of mutations would probably destroy the central β-strand pairing of the TAG-$1_{Ig1–4}$ dimer. First, deletion of the residues corresponding to chicken Ile^{187}–Ile^{190} in human TAG-1 would eliminate the dimerizing part of the Ig2 G strand by shortening the FG β-loop. The hydrophobic interaction of Phe^{185} with the hydrophobic pocket of the dimer mate would also be abolished. Second, a double alanine mutation of His^{182} and Phe^{185} would abolish the hydrophobic interaction of Phe^{185} with the hydrophobic pocket or disturb the geometry of the whole FG β-loop, because of a stabilizing effect of the hydrogen bond of His^{182} to Ser^{135} in the human ortholog. Although the corresponding His^{186} in chicken TAG-$1_{Ig1–4}$ does not form a hydrogen bond with the corresponding Ser^{139}, but with the main-chain carbonyl of Glu^{188} (see Fig. 3B), the conformation of the FG loop is similar to that observed in the human TAG-$1_{Ig1–4}$ structure. Since there are no single alanine mutants, it is unknown if either the histidine or the phenylalanine residue is important for homophilic interaction alone or together. Analysis of the largest lattice contact as well as detailed analysis of the Ig2 FG loop strongly suggest that this Ig2 FG loop is involved in a homophilic interaction mechanism.

TAG-1 protein interaction site is in accordance with other experiments

We propose that the characteristic of TAG-1 dimerization is a groove to groove interaction of the Ig1/Ig2 domains, which requires a correct angular orientation of the rigid groups Ig1:Ig4 and Ig2:Ig3 with respect to the hinge axis, and that TAG-1 dimer stability results from the hydrophobic interaction of the Phe^{185} side chain with the hydrophobic pocket of the dimer mate and from intermolecular β-strand pairing of the Ig2 G strands. Therefore, the proposed dimerization of TAG-1 may involve an induced fit mechanism (Koshland 1958), requiring domain flexibility between Ig1 and Ig2 and small side-chain readjustments within the FG loop of the Ig2 domain during dimer formation.

The observed crystallographic dimer of two human TAG-$1_{Ig1–4}$ molecules thus may promote a homophilic *trans* interaction in vivo. This contradicts with the zipper model proposed for the chicken ortholog, because in human TAG-1 both dimer mates interact with identical surface sites, namely, the G strands located at the Ig1–Ig2 groove, whereas the proposed zipper units of the chicken ortholog contact each other via different surface sites, the Ig2 FG loop of one molecule and the extended Ig3 CE loop of a second TAG-1 molecule. Another zipper-based mechanism was proposed for cell–cell adhesion mediated by cadherins, which involves twofold crystallographic symmetry between all molecular *cis* and *trans* contacts of the proposed zipper (Shapiro et al. 1995).

In the case of human TAG-1, S2 cell–cell aggregation via the FnIII domains has been reported (Tsiotra et al. 1996). Antibody mapping experiments, in combination with myeloma cell–cell interaction studies, had narrowed down the importance of the FnIII domains to the fourth domain, for TAG-1 induced cell–cell interaction (Kunz et al. 2002). These findings led to an extended zipper model, where *trans*-interacting TAG-1 molecules forming a zipper, also interact with their FnIII domains in *cis*, by dimer formation via the fourth FnIII domain (see Fig. 5 in Kunz et al. 2002). There are no experiments which show that the *cis* interaction of TAG-1 needs a preformed "*trans* zipper" or that TAG-1 molecules forming a homodimer but not a zipper cannot interact in *cis* via its FnIII domains with other TAG-1 molecules. It is also not known, whether TAG-1 molecules can interact in *cis* without interacting simultaneously in *trans*. It is known however, that blocking of TAG-1 mediated myeloma cell–cell aggregation is possible using monoclonal antibodies against the four N-terminal Ig-domains, or the fourth FnIII domain (Kunz et al. 2002). This suggests that homophilic cell–cell aggregation by TAG-1 can only occur, if at least some of the involved TAG-1 molecules bind other TAG-1 molecules located in *cis* and *trans* simultaneously.

Multiple molecule mode and the four molecule mode

On the basis of the proposed interaction sites of human TAG-1, a new mode of homophilic cell–cell interaction can be proposed.

In *multiple molecule mode* (see Fig. 4C), each TAG-1 molecule participates with its $Ig_{1–4}$ binding module in a *trans* dimer with a second TAG-1 molecule and with its fourth FnIII domain in a *cis* dimer with a third TAG-1 molecule (see Fig. 4C).

The resulting unbranched, curvilinear string of connected TAG-1 molecules somehow resembles the already proposed zipper mode (cf. Fig. 4A and Kunz et al. 2002), but it does not allow for a two-dimensional network of TAG-1 molecules at the contact interface of two interacting cells.

Within this framework, cyclic strings formed by only four molecules are feasible involving simultaneous *cis*

and *trans* interactions of each participating molecule (see Fig. 4B). The formation of *trans–cis* complexes of the *multiple molecule* string and the *four molecule* cyclic string can occur stepwise. In a first aggregation event, the *cis* interaction of the two FnIII domains can be established followed by *trans* association of the binding modules. It was observed that chicken TAG-1 adopts a back-folded conformation, where the four N-terminal Ig domains are located toward the membrane in close proximity to the FnIII domains (Rader et al. 1993). Back-folded TAG-1 molecules can probably interact with already *trans* dimerized molecules with their fourth FnIII, which could induce the release of the ligand-binding module from the back-folded orientation onto an orientation toward the subsequent *trans* interaction partner, a TAG-1 molecule presented by a neighboring cell.

Additional arguments based on experimental evidence are required to allow a decision in favor of one among the currently possible interaction modes, the *multiple molecule mode*, or the zipper mode and to reject the remaining ones.

Materials and Methods

Expression and purification of TAG-$1_{Ig1–4}$

DNA coding for the four N-terminal Ig domains of TAG-$1_{Ig1–4}$ (residues 28–418) was cloned into the vector pET15b (Novagen). The construct contained one extra N-terminal amino acid (M) and eight extra C-terminal amino acids containing a hexahistidine tag (RSHHHHHH). Expression was carried out in *Escherichia coli* strain BL21 (DE3) pRILP (Novagen) using a medium containing 10 g of *N-Z*-amine A (Sigma), 5 g of yeast extract (Fluka), and 7.5 g of NaCl (Sigma) per liter at 37°C. Protein expression was induced at an optical density of 0.9 at 600 nm with 1 mM isopropyl-β-D-thiogalactopyranoside (Fermentas). Three hours after induction, cells were harvested by centrifugation at 10,000*g* for 3 min, and cell pellets were resuspended in distilled water and broken using a continuous cell-disruption system (Constant Systems Ltd.), at 2.5 kbar. Inclusion bodies were washed by three cycles of centrifugation and resuspension with distilled water and solubilized by overnight incubation with 8 M urea (Sigma), 100 mM Tris-HCl (Fluka), pH 8.5, 320 mM NaCl, 50 mM 2-mercaptoethanol (Fluka) (solubilization buffer) at room temperature. The solute was centrifuged for 2 h at 75,000*g*, and the supernatant was filtered through a 0.22-μm filter and purified using a 4-mL HisTrap HP column (GE Healthcare) using the following protocol at a flow rate of 0.5 mL/cm^2: (1) column equilibration with 3 column volumes (CV) of solubilization buffer containing 20 mM 2-mercaptoethanol; (2) application of denatured TAG-1 to the column; (3) washing step I—3 CV of equilibration buffer; (4) washing step II—3 CV of solubilization buffer; and (5) elution with washing buffer II containing 0.25 M imidazole (Fluka).

Refolding and purification of renatured TAG-$1_{Ig1–4}$

Prior to refolding, the concentration of denatured TAG-$1_{Ig1–4}$ was adjusted to 4 mg/mL in elution buffer and DL-cysteine (Fluka) was added to a final concentration of 200 mM. TAG-$1_{Ig1–4}$ was refolded using a quick dilution method into a buffer containing 0.8 M L-arginine (Fluka), 100 mM Tris-HCl, pH 8.5, and 320 mM NaCl. The final TAG-$1_{Ig1–4}$ concentration during refolding was 40 mg/L. Dilution and refolding was carried out at 4°C in 100-mL aliquots. The success of TAG-$1_{Ig1–4}$ refolding was monitored by comparing the apparent molecular weight after SDS/PAGE (Laemmli 1970) under reducing and nonreducing conditions.

Fully oxidized and refolded TAG-$1_{Ig1–4}$ was concentrated 500-fold using an Amicon ultrafiltration unit with a YM10 membrane (Millipore) followed by a Vivaspin centrifugation filter (Vivascience GmbH), both with 10-kDa molecular weight cutoffs. Concentrated TAG-$1_{Ig1–4}$ was subjected to size-exclusion chromatography with Superdex 200 (GE Healthcare) at a flow rate of 0.5 mL/cm^2 with a running buffer containing 20 mM Tris-HCl, pH 8.5, and 150 mM NaCl. TAG-1 protein concentration in all experimental steps was determined as described (Gill and von Hippel 1989).

Crystallization, data collection, phasing, and structure refinement

Human TAG-$1_{Ig1–4}$ was crystallized using the sitting-drop method by mixing 100 nL of protein solution (4 mg/mL) and 100 nL of crystallization buffer (12% polyethylene glycol 20000 [Fluka], 100 mM Tris-HCl pH 8.5, 200 mM KCl [Sigma]). Pipetting was done using an automatic liquid handling system (Cartesian Dispensing Systems, Genomic Solutions). Needle-shaped crystals were transferred into a drop containing 80% (v/v) of the crystallization buffer supplemented with 20% (v/v) ethylene glycol (Sigma) for 5 min prior to flash freezing in a 100°K cryostream (Oxford Cryosystems Ltd.). Diffraction data were collected at the X06SA beamline of the Swiss Light Source (Paul Scherrer Institut, Villigen, Switzerland). All diffraction images were processed using the program XDS (Kabsch 1993). Phases were determined with the molecular replacement program MOLREP (Vagin and Teplyakov 1997) and chicken TAG-1 as search model (PDB code 1CS6). The solution obtained was improved by 30 cycles of rigid-body refinement with REFMAC (Collaborative Computational Project, Number 4 1994). The final model was obtained after several cycles of manual model building using COOT (Emsley and Cowtan 2004) and restrained refinement with REFMAC using separate anisotropic temperature factor tensors (TLS) (Winn et al. 2001) for each Ig domain.

Accession numbers

The coordinates and the structure factors of TAG-$1_{Ig1–4}$ have been deposited with the Protein Data Bank (Berman et al. 2000) under accession code 2OM5.

Analysis of intermolecular interactions

The total buried surface value (B) of the TAG-1 dimer interfaces, the nonpolar interface area ($f_{np}B$), the fraction of fully buried atoms (f_{bu}), and the residue propensity score (RP) were calculated by a Web-based server (http://resources.boseinst.ernet.in/resources/bioinfo/interface) (Saha et al. 2006). All parameter definitions have been published (Bahadur et al. 2004). The shape complementarity value (S_C) was calculated

by the program SC (Lawrence and Colman 1993), which is part of the CCP4 software package (Collaborative Computational Project Number 4 1994).

Acknowledgments

This work was supported by the Deutsche Forschungsgemeinschaft (TR SFB 11). We gratefully acknowledge the help of the SLS beamline X06SA staff.

References

Alvarez-Dolado, M., Figueroa, A., Kozlov, S., Sonderegger, P., Furley, A.J., and Muñoz, A. 2001. Thyroid hormone regulates TAG-1 expression in the developing rat brain. *Eur. J. Neurosci.* **14:** 1209–1218.

Bahadur, R.P., Chakrabarti, P., Rodier, F., and Janin, J. 2004. A dissection of specific and non-specific protein–protein interfaces. *J. Mol. Biol.* **336:** 943–955.

Berman, H.M., Westbrook, J., Feng, Z., Gilliland, G., Bhat, T.N., Weissig, H., Shindyalov, I.N., and Bourne, P.E. 2000. The Protein Data Bank. *Nucleic Acids Res.* **28:** 235–242.

Brümmendorf, T. and Rathjen, F.G. 1996. Structure/function relationships of axon-associated adhesion receptors of the immunoglobulin superfamily. *Curr. Opin. Neurobiol.* **6:** 584–593.

Buchstaller, A., Kunz, S., Berger, P., Kunz, B., Ziegler, U., Rader, C., and Sonderegger, P. 1996. Cell adhesion molecules NgCAM and axonin-1 form heterodimers in the neuronal membrane and cooperate in neurite outgrowth promotion. *J. Cell Biol.* **135:** 1593–1607.

Burgoon, M.P., Grumet, M., Mauro, V., Edelman, G.M., and Cunningham, B.A. 1991. Structure of the chicken neuron-glia cell adhesion molecule, Ng-CAM: Origin of the polypeptides and relation to the Ig superfamily. *J. Cell Biol.* **112:** 1017–1029.

Burley, S.K. and Petsko, G.A. 1985. Aromatic–aromatic interaction: A mechanism of protein structure stabilization. *Science* **229:** 23–28.

Buttiglione, M., Revest, J.M., Pavlou, O., Karagogeos, D., Furley, A., Rougon, G., and Faivre-Sarrailh, C. 1998. A functional interaction between the neuronal adhesion molecules TAG-1 and F3 modulates neurite outgrowth and fasciculation of cerebellar granule cells. *J. Neurosci.* **18:** 6853–6870.

Chothia, C. and Jones, E.Y. 1997. The molecular structure of cell adhesion molecules. *Annu. Rev. Biochem.* **66:** 823–862.

Collaborative Computational Project, Number 4. 1994. The CCP4 suite: Programs for protein crystallography. *Acta Crystallogr. D Biol. Crystallogr.* **50:** 760–763.

De Angelis, E., MacFarlane, J., Du, J.S., Yeo, G., Hicks, R., Rathjen, F.G., Kenwrick, S., and Brümmendorf, T. 1999. Pathological missense mutations of neural cell adhesion molecule L1 affect homophilic and heterophilic binding activities. *EMBO J.* **18:** 4744–4753.

Denaxa, M., Chan, C.H., Schachner, M., Parnavelas, J.G., and Karagogeos, D. 2001. The adhesion molecule TAG-1 mediates the migration of cortical interneurons from the ganglionic eminence along the corticofugal fiber system. *Development* **128:** 4635–4644.

Diederichs, K. and Karplus, P.A. 1997. Improved *R*-factors for diffraction data analysis in macromolecular crystallography. *Nat. Struct. Biol.* **4:** 269–275.

Dodd, J. and Jessell, T.M. 1988. Axon guidance and the patterning of neuronal projections in vertebrates. *Science* **242:** 692–699.

Dodd, J., Morton, S.B., Karagogeos, D., Yamamoto, M., and Jessell, T.M. 1988. Spatial regulation of axonal glycoprotein expression on subsets of embryonic spinal neurons. *Neuron* **1:** 105–116.

Emsley, P. and Cowtan, K. 2004. COOT: Model-building tools for molecular graphics. *Acta Crystallogr. D Biol. Crystallogr.* **60:** 2126–2132.

Felsenfeld, D.P., Hynes, M.A., Skoler, K.M., Furley, A.J., and Jessell, T.M. 1994. TAG-1 can mediate homophilic binding, but neurite outgrowth on TAG-1 requires an L1-like molecule and β1 integrins. *Neuron* **12:** 675–690.

Fitzli, D., Stoeckli, E.T., Kunz, S., Siribour, K., Rader, C., Kunz, B., Kozlov, S.V., Buchstaller, A., Lane, R.P., Suter, D.M., et al. 2000. A direct interaction of axonin-1 with NgCAM-related cell adhesion molecule (NrCAM) results in guidance, but not growth of commissural axons. *J. Cell Biol.* **149:** 951–968.

Freigang, J., Proba, K., Leder, L., Diederichs, K., Sonderegger, P., and Welte, W. 2000. The crystal structure of the ligand binding module of axonin-1/TAG-1 suggests a zipper mechanism for neural cell adhesion. *Cell* **101:** 425–433.

Gill, S.C. and von Hippel, P.H. 1989. Calculation of protein extinction coefficients from amino acid sequence data. *Anal. Biochem.* **182:** 319–326.

Grumet, M. and Edelman, G.M. 1984. Heterotypic binding between neuronal membrane vesicles and glial cells is mediated by a specific cell adhesion molecule. *J. Cell Biol.* **98:** 1746–1756.

Grumet, M., Mauro, V., Burgoon, M.P., Edelman, G.M., and Cunningham, B.A. 1991. Structure of a new nervous system glycoprotein, Nr-CAM, and its relationship to subgroups of neural cell adhesion molecules. *J. Cell Biol.* **113:** 1399–1412.

Hasler, T.H., Rader, C., Stoeckli, E.T., Zuellig, R.A., and Sonderegger, P. 1993. cDNA cloning, structural features, and eucaryotic expression of human TAG-1/axonin-1. *Eur. J. Biochem.* **211:** 329–339.

Hayward, S. and Lee, R.A. 2002. Improvements in the analysis of domain motions in proteins from conformational change: DynDom version 1.50. *J. Mol. Graph. Model.* **21:** 181–183.

Hynes, R.O. and Lander, A.D. 1992. Contact and adhesive specificities in the associations, migrations, and targeting of cells and axons. *Cell* **68:** 303–322.

Janin, J. 1997. Specific versus non-specific contacts in protein crystals. *Nat. Struct. Biol.* **4:** 973–974.

Janin, J. and Rodier, F. 1995. Protein–protein interaction at crystal contacts. *Proteins* **23:** 580–587.

Jessell, T.M. 1988. Adhesion molecules and the hierarchy of neural development. *Neuron* **1:** 3–13.

Kabsch, W. 1993. Automatic processing of rotation diffraction data from crystals of initially unknown symmetry and cell constants. *J. Appl. Crystallogr.* **26:** 795–800.

Karagogeos, D., Morton, S.B., Casano, F., Dodd, J., and Jessell, T.M. 1991. Developmental expression of the axonal glycoprotein TAG-1: Differential regulation by central and peripheral neurons in vitro. *Development* **112:** 51–67.

Koshland, D.E. 1958. Application of a theory of enzyme specificity to protein synthesis. *Proc. Natl. Acad. Sci.* **44:** 98–104.

Kraulis, P.J. 1991. MOLSCRIPT: A program to produce both detailed and schematic plots of protein structures. *J. Appl. Crystallogr.* **24:** 946–950.

Kuhn, T.B., Stoeckli, E.T., Condrau, M.A., Rathjen, F.G., and Sonderegger, P. 1991. Neurite outgrowth on immobilized axonin-1 is mediated by a heterophilic interaction with L1(G4). *J. Cell Biol.* **115:** 1113–1126.

Kunz, B., Lierheimer, R., Rader, C., Spirig, M., Ziegler, U., and Sonderegger, P. 2002. Axonin-1/TAG-1 mediates cell–cell adhesion by a *cis*-assisted *trans*-interaction. *J. Biol. Chem.* **277:** 4551–4557.

Kunz, S., Spirig, M., Ginsburg, C., Buchstaller, A., Berger, P., Lanz, R., Rader, C., Vogt, L., Kunz, B., and Sonderegger, P. 1998. Neurite fasciculation mediated by complexes of axonin-1 and Ng cell adhesion molecule. *J. Cell Biol.* **143:** 1673–1690.

Laemmli, U.K. 1970. Cleavage of structural proteins during the assembly of the head of bacteriophage T4. *Nature* **227:** 680–685.

Laskowski, R.A., MacArthur, M.W., Moss, D.S., and Thornton, J.M. 1993. PROCHECK: A program to check the stereochemical quality of protein structures. *J. Appl. Crystallogr.* **26:** 283–291.

Lawrence, M.C. and Colman, P.M. 1993. Shape complementarity at protein/protein interfaces. *J. Mol. Biol.* **234:** 946–950.

Lemmon, V., Farr, K.L., and Lagenaur, C. 1989. L1-mediated axon outgrowth occurs via a homophilic binding mechanism. *Neuron* **2:** 1597–1603.

Lustig, M., Sakurai, T., and Grumet, M. 1999. Nr-CAM promotes neurite outgrowth from peripheral ganglia by a mechanism involving axonin-1 as a neuronal receptor. *Dev. Biol.* **209:** 340–351.

Malhotra, J.D., Tsiotra, P., Karagogeos, D., and Hortsch, M. 1998. *Cis*-activation of L1-mediated ankyrin recruitment by TAG-1 homophilic cell adhesion. *J. Biol. Chem.* **273:** 33354–33359.

Merritt, E.A. and Bacon, D.J. 1997. Raster3D: Photorealistic molecular graphics. *Methods Enzymol.* **277:** 505–524.

Milev, P., Maurel, P., Häring, M., Margolis, R.K., and Margolis, R.U. 1996. TAG-1/axonin-1 is a high-affinity ligand of neurocan, phosphacan/protein-tyrosine phosphatase-ζ/β, and N-CAM. *J. Biol. Chem.* **271:** 15716–15723.

Moos, M., Tacke, R., Scherer, H., Teplow, D., Früh, K., and Schachner, M. 1988. Neural adhesion molecule L1 as a member of the immunoglobulin superfamily with binding domains similar to fibronectin. *Nature* **334:** 701–703.

Pavlou, O., Theodorakis, K., Falk, J., Kutsche, M., Schachner, M., Faivre-Sarrailh, C., and Karagogeos, D. 2002. Analysis of interactions of the adhesion molecule TAG-1 and its domains with other immunoglobulin superfamily members. *Mol. Cell. Neurosci.* **20:** 367–381.

Rader, C., Stoeckli, E.T., Ziegler, U., Osterwalder, T., Kunz, B., and Sonderegger, P. 1993. Cell–cell adhesion by homophilic interaction of

the neuronal recognition molecule axonin-1. *Eur. J. Biochem.* **215:** 133–141.

Rader, C., Kunz, B., Lierheimer, R., Giger, R.J., Berger, P., Tittmann, P., Gross, H., and Sonderegger, P. 1996. Implications for the domain arrangement of axonin-1 derived from the mapping of its NgCAM binding site. *EMBO J.* **15:** 2056–2068.

Rathjen, F.G. and Jessell, T.M. 1991. Glycoproteins that regulate the growth and guidance of vertebrate axons: Domains and dynamics of the immunoglobulin/fibronectin type III subfamily. *Semin. Neurosci.* **3:** 297–307.

Rickman, D.S., Tyagi, R., Zhu, X.X., Bobek, M.P., Song, S., Blaivas, M., Misek, D.E., Israel, M.A., Kurnit, D.M., Ross, D.A., et al. 2001. The gene for the axonal cell adhesion molecule TAX-1 is amplified and aberrantly expressed in malignant gliomas. *Cancer Res.* **61:** 2162–2168.

Saha, R., Bahadur, R., Pal, A., Mandal, S., and Chakrabarti, P. 2006. ProFace: A server for the analysis of the physicochemical features of protein–protein interfaces. *BMC Struct. Biol.* **6:** 11. doi: 10.1186/1472-6807-6-11.

Schürmann, G., Haspel, J., Grumet, M., and Erickson, H.P. 2001. Cell adhesion molecule L1 in folded (horseshoe) and extended conformations. *Mol. Biol. Cell* **12:** 1765–1773.

Shapiro, L., Fannon, A.M., Kwong, P.D., Thompson, A., Lehmann, M.S., Grübel, G., Legrand, J.F., Als-Nielsen, J., Colman, D.R., and Hendrickson, W.A. 1995. Structural basis of cell–cell adhesion by cadherins. *Nature* **374:** 327–337.

Stoeckli, E.T., Lemkin, P.F., Kuhn, T.B., Ruegg, M.A., Heller, M., and Sonderegger, P. 1989. Identification of proteins secreted from axons of embryonic dorsal-root-ganglia neurons. *Eur. J. Biochem.* **180:** 249–258.

Stoeckli, E.T., Kuhn, T.B., Duc, C.O., Ruegg, M.A., and Sonderegger, P. 1991. The axonally secreted protein axonin-1 is a potent substratum for neurite growth. *J. Cell Biol.* **112:** 449–455.

Su, X.D., Gastinel, L.N., Vaughn, D.E., Faye, I., Poon, P., and Bjorkman, P.J. 1998. Crystal structure of hemolin: A horseshoe shape with implications for homophilic adhesion. *Science* **281:** 991–995.

Suter, D.M., Pollerberg, G.E., Buchstaller, A., Giger, R.J., Dreyer, W.J., and Sonderegger, P. 1995. Binding between the neural cell adhesion molecules axonin-1 and Nr-CAM/Bravo is involved in neuron–glia interaction. *J. Cell Biol.* **131:** 1067–1081.

Tessier-Lavigne, M. and Goodman, C.S. 1996. The molecular biology of axon guidance. *Science* **274:** 1123–1133.

Traka, M., Dupree, J.L., Popko, B., and Karagogeos, D. 2002. The neuronal adhesion protein TAG-1 is expressed by Schwann cells and oligodendrocytes and is localized to the juxtaparanodal region of myelinated fibers. *J. Neurosci.* **22:** 3016–3024.

Tsiotra, P.C., Karagogeos, D., Theodorakis, K., Michaelidis, T.M., Modi, W.S., Furley, A.J., Jessell, T.M., and Papamatheakis, J. 1993. Isolation of the cDNA and chromosomal localization of the gene (TAX1) encoding the human axonal glycoprotein TAG-1. *Genomics* **18:** 562–567.

Tsiotra, P.C., Theodorakis, K., Papamatheakis, J., and Karagogeos, D. 1996. The fibronectin domains of the neural adhesion molecule TAX-1 are necessary and sufficient for homophilic binding. *J. Biol. Chem.* **271:** 29216–29222.

Vagin, A. and Teplyakov, A. 1997. MOLREP: An automated program for molecular replacement. *J. Appl. Crystallogr.* **30:** 1022–1025.

Winn, M.D., Isupov, M.N., and Murshudov, G.N. 2001. Use of TLS parameters to model anisotropic displacements in macromolecular refinement. *Acta Crystallogr. D Biol. Crystallogr.* **57:** 122–133.

Yamamoto, M., Boyer, A.M., Crandall, J.E., Edwards, M., and Tanaka, H. 1986. Distribution of stage-specific neurite-associated proteins in the developing murine nervous system recognized by a monoclonal antibody. *J. Neurosci.* **6:** 3576–3594.